

Digital Quantum Simulation of the Schwinger Model with Topological Term via Adiabatic State Preparation

Bipasha Chakraborty,^{1,*} Masazumi Honda,^{1,†} Taku Izubuchi,^{2,3,‡} Yuta Kikuchi,^{3,§} and Akio Tomiya^{3,¶}

¹*Department of Applied Mathematics and Theoretical Physics,*

Centre for Mathematical Sciences, Wilberforce Road, Cambridge, CB3 0WA, UK

²*Physics Department, Brookhaven National Laboratory, Upton, New York 11973, USA*

³*RIKEN BNL Research center, Brookhaven National Laboratory, Upton, NY, 11973, USA*

(Dated: February 26, 2020)

We perform a digital quantum simulation of a gauge theory with a topological term in Minkowski spacetime, which is practically inaccessible by standard lattice Monte Carlo simulations. We focus on $1+1$ dimensional quantum electrodynamics with the θ -term known as the Schwinger model. We construct the true vacuum state of a lattice Schwinger model using adiabatic state preparation which, in turn, allows us to compute an expectation value of the fermion mass operator with respect to the vacuum. Upon taking a continuum limit we find that our result in massless case agrees with the known exact result. In massive case, we find an agreement with mass perturbation theory in small mass regime and deviations in large mass regime. We estimate computational costs required to take a reasonable continuum limit. Our results imply that digital quantum simulation is already useful tool to explore non-perturbative aspects of gauge theories with real time and topological terms.

I. INTRODUCTION

Gauge theory plays a central role in understanding our universe as all the known fundamental forces are described in the framework of gauge theory. Quantum Chromodynamics (QCD) is the gauge theory describing the strong interaction among quarks and gluons. Since QCD is asymptotically free, we need a non-perturbative treatment at low-energy to interpolate perturbative picture of quarks/gluons and physics of hadrons. The only successful first-principle approach to handle this is lattice QCD in which we conventionally consider QCD on 4d Euclidean spacetime and discretize the spacetime by lattice to make the path integral finite dimensional. Evaluating the regularized path integral numerically and taking the large volume and continuum limits carefully, one can study non-perturbative phenomena such as confinement and chiral symmetry breaking, and reproduce correct hadron spectrum [1–4]. Numerical integration of path integral in lattice field theory is commonly performed by the Markov-Chain Monte Carlo method which uses Boltzmann weight as a generating probability of samples. This leads a problem when the integrand is non-real positive and highly oscillating, and the sampling becomes much less efficient. This problem known as the sign prob-

lem physically happens *e.g.* when we have topological terms [5], chemical potentials [6] or real time dynamics [7]. All of the above cases are crucial to understand our universe and therefore, an efficient way to explore the above situations is highly demanded [3–7].

There are various approaches to challenge the sign problem within the framework of path integral formalism [6]; however, with limited success as the sign problem gets more serious. One way to address the problem is to attack gauge theories with the sign problem by switching to Hamiltonian formalism where the sign problem is absent from the beginning. In return, one needs to regularize infinite dimensional Hilbert space and deal with huge vector space whose dimension is typically exponential of the regularized degrees of freedom. It seems beyond the capacity of current/near-future supercomputers when spacetime dimension is not low. However, it is reasonable to expect that *quantum computers* do this job in the not-so-distant-future. Anticipating growth of quantum computational resources, it is worth to develop methods to analyze gauge theories suitable for quantum computers to prepare for the coming era of quantum supremacy [8, 9]. It is particularly important to identify suitable algorithms and estimate computational resources required to take a reasonable continuum limit.

In this letter, we implement a *digital quantum simulation* of a gauge theory with a topological term on Minkowski spacetime which is practically inaccessible by the standard Monte Carlo approach. We focus on the Schwinger model with the θ -term [10–13], which is $1+1$ dimensional $U(1)$ gauge theory coupled to a Dirac

*bc335ATdamtp.cam.ac.uk

†mh974ATdamtp.cam.ac.uk

‡izubuchiATquark.phy.bnl.gov

§yuta.kikuchiATriken.jp

¶akio.tomiyaATriken.jp

fermion described by the Lagrangian,

$$\mathcal{L}_0 = -\frac{1}{4}F_{\mu\nu}F^{\mu\nu} + \frac{g\theta}{4\pi}\epsilon_{\mu\nu}F^{\mu\nu} + i\bar{\psi}\gamma^\mu(\partial_\mu + igA_\mu)\psi - m\bar{\psi}\psi, \quad (1)$$

where $\gamma^0 = \sigma^3$, $\gamma^1 = i\sigma^2$, $\gamma^5 = \gamma^0\gamma^1$ and $F_{\mu\nu} = \partial_\mu A_\nu - \partial_\nu A_\mu$. The physical parameters of this model are the gauge coupling g , topological angle θ , and fermion mass m . We discretize the space by lattice keeping time continuous and work in Hamiltonian formalism. Then we construct the true vacuum of the lattice Schwinger model at finite (g, θ, m) by a digital quantum simulation via adiabatic state preparation and compute the vacuum expectation value (VEV) of the fermion mass operator $\bar{\psi}\psi$. We take the infinite volume and continuum limits and find that our result in massless case agrees with the exact result known in literature [14–17]. In massive case, we find an agreement with mass perturbation theory [18, 19] for small m and deviations for large m [65]. Our results imply that digital quantum simulation is already useful tool to explore non-perturbative aspects of gauge theories with topological terms on Minkowski spacetime even in current computational resource. Here we use a quantum simulator rather than real quantum computers for the purpose of designing quantum algorithms for gauge theories. Its implementations on a real quantum device is left as a future work, that is another vital task especially in the forthcoming Noisy Intermediate-Scale Quantum (NISQ) era [20].

Many efforts have already been made on designing and implementing digital quantum simulations of quantum field theories [21–41] as well as analog quantum simulations [42–55]. In particular, the Schwinger model provides an ideal laboratory for developing quantum algorithms with limited quantum resources foreseeing larger-scale digital quantum simulations of various gauge theories. So far, the digital quantum simulations of the Schwinger model are limited to $\theta = 0$, and performed with a free vacuum and quenching evolution [28, 29, 33, 39, 56] while analogue quantum simulations have been implemented in [51, 55]. The present work demonstrates how to construct the true vacuum in an interacting gauge theory with the topological term by a digital quantum simulation. We believe that our results open up potential applications of digital quantum simulation to quantum field theory since the preparation of true ground state is an indispensable step to calculate various observables such as scattering amplitudes non-perturbatively¹.

II. SCHWINGER MODEL AS QUBITS

First, we rewrite the lattice Schwinger model in terms of spin operators which act on the Hilbert space represented by qubits according to [59]. Instead of directly analyzing the system with the Lagrangian (1), we consider the Lagrangian obtained by the chiral rotation $\psi \rightarrow e^{i\frac{\theta}{2}\gamma^5}\psi$ to absorb the θ -term via the transformation of the path integral measure [60]. Therefore, we can study the same physics by the Lagrangian,

$$\mathcal{L} = -\frac{1}{4}F_{\mu\nu}F^{\mu\nu} + i\bar{\psi}\gamma^\mu(\partial_\mu + igA_\mu)\psi - m\bar{\psi}e^{i\theta\gamma^5}\psi. \quad (2)$$

In the temporal gauge $A_0 = 0$, the Hamiltonian of this model is

$$H = \int dx \left[-i\bar{\psi}\gamma^1(\partial_1 + igA_1)\psi + m\bar{\psi}\psi + \frac{1}{2}\Pi^2 \right], \quad (3)$$

where $\Pi \equiv \dot{A}^1$ is the conjugate momentum of A^1 . The gauge invariance of physical Hilbert space is guaranteed by imposing the Gauss law:

$$0 = -\partial_1\Pi - g\bar{\psi}\gamma^0\psi. \quad (4)$$

A. Lattice theory with Staggered fermion

To implement a quantum simulation, we need a regularization to make the Hilbert space finite dimensional. For the Schwinger model, this is done just by placing the theory on a lattice and imposing the Gauss law² [29]. Let us consider the theory on 1d spatial lattice with N sites and lattice spacing a keeping the time continuous. Using the staggered fermion [61, 62], the lattice Hamiltonian is given by³

$$H = -i \sum_{n=1}^{N-1} \left(w - (-1)^n \frac{m}{2} \sin \theta \right) \left[\chi_n^\dagger e^{i\phi_n} \chi_{n+1} - \text{h.c.} \right] + m \cos \theta \sum_{n=1}^N (-1)^n \chi_n^\dagger \chi_n + J \sum_{n=1}^{N-1} L_n^2, \quad (5)$$

where $w = 1/(2a)$ and $J = g^2 a/2$. We have rescaled the gauge operators as $\phi_n \leftrightarrow -agA^1(x)$ and $L_n \leftrightarrow -\Pi(x)/g$, where ϕ_n lives on a site n while L_n lives on a link between sites n and $n+1$. A two-component Dirac fermion $\psi(x) = (\psi_u(x), \psi_d(x))^\top$ is translated into a pair of neighboring

¹ Schwinger model with the θ -term has been studied by other approaches without using quantum computing in [57, 58].

² This is true for open boundary condition while there is a remaining gauge degree of freedom for periodic boundary condition.

³ Note that staggered fermion in 1 + 1 dimensions in Hamilton formalism has only one taste.

one-component fermions according to the correspondence (see Appendix A for details):

$$\frac{\chi_n}{\sqrt{a}} \leftrightarrow \begin{cases} \psi_u(x) & n : \text{even} \\ \psi_d(x) & n : \text{odd} \end{cases}. \quad (6)$$

They satisfy the (anti-)commutation relations

$$\{\chi_n^\dagger, \chi_m\} = \delta_{mn}, \quad \{\chi_n, \chi_m\} = 0, \quad [\phi_n, L_m] = i\delta_{mn}, \quad (7)$$

and the Gauss law on the lattice is

$$L_n - L_{n-1} = \chi_n^\dagger \chi_n - \frac{1 - (-1)^n}{2}. \quad (8)$$

B. Mapping to spin system

We rewrite the system in terms of spin variables in three steps. Firstly, we perform the Jordan-Wigner transformation [63], which maps the fermions to spin variables as

$$\chi_n = \left(\prod_{\ell < n} iZ_\ell \right) \frac{X_n - iY_n}{2}, \quad (9)$$

where (X_n, Y_n, Z_n) stands for the Pauli matrices $(\sigma^1, \sigma^2, \sigma^3)$ at site n . Secondly, we specify a boundary condition and solve the Gauss law. We impose an open boundary condition which restricts L_n to a constant at the boundary. Solving the Gauss law, we rewrite L_n in terms of the spin variables as

$$L_n = L_0 + \frac{1}{2} \sum_{\ell=1}^n (Z_\ell + (-1)^\ell), \quad (10)$$

where the constant L_0 specifies our boundary condition. The Schwinger model with (θ, L_0) is equivalent to the one with $(\theta + 2\pi L_0, 0)$ [12] and therefore we can take $L_0 = 0$ without loss of generality. Finally, we can eliminate ϕ_n by the redefinition⁴ $\chi_n \rightarrow \prod_{\ell < n} [e^{-i\phi_\ell}] \chi_n$.

Thus, the lattice Schwinger model is described only in terms of the spin variables:

$$H = H_{ZZ} + H_\pm + H_Z, \quad (11)$$

where

$$H_{ZZ} = \frac{J}{2} \sum_{n=2}^J \sum_{1 \leq k < \ell \leq n} Z_k Z_\ell,$$

$$H_\pm = \frac{1}{2} \sum_{n=1}^{N-1} \left(w - (-1)^n \frac{m}{2} \sin \theta \right) [X_n X_{n+1} + Y_n Y_{n+1}],$$

$$H_Z = \frac{m \cos \theta}{2} \sum_{n=1}^N (-1)^n Z_n - \frac{J}{2} \sum_{n=1}^{N-1} (n \bmod 2) \sum_{\ell=1}^n Z_\ell, \quad (12)$$

up to irrelevant constant terms. Note that the nonlocal interactions in H_{ZZ} show up as a consequence of solving the Gauss law constraint. For the alternative formulation of θ term by directly discretizing (1) before using the anomaly relation, see appendix B.

III. ADIABATIC PREPARATION OF VACUUM

We study the VEV of the mass operator:

$$\langle \bar{\psi}(x)\psi(x) \rangle = \langle \text{vac} | \bar{\psi}(x)\psi(x) | \text{vac} \rangle, \quad (13)$$

where $|\text{vac}\rangle$ is the ground state of the full Hamiltonian H . Here, instead of directly studying the local operator $\bar{\psi}(x)\psi(x)$, we analyze the operator averaged over space:

$$\frac{1}{2Na} \langle \text{vac} | \sum_{n=1}^N (-1)^n Z_n | \text{vac} \rangle, \quad (14)$$

whose infinite volume limit is the same as $\langle \bar{\psi}(x)\psi(x) \rangle$ by translational invariance.

We prepare the vacuum state $|\text{vac}\rangle$ using the adiabatic theorem as follows. We first choose an initial Hamiltonian H_0 of a simple system such that its ground state $|\text{vac}\rangle_0$ is unique and known. Next, we consider the following time evolution of $|\text{vac}\rangle_0$:

$$\mathcal{T} \exp \left(-i \int_0^T dt H_A(t) \right) |\text{vac}\rangle_0, \quad (15)$$

where $\mathcal{T} \exp$ denotes a time-ordered exponential. The adiabatic Hamiltonian $H_A(t)$ is an hermitian operator satisfying

$$H_A(0) = H_0, \quad H_A(T) = H. \quad (16)$$

The adiabatic theorem claims that, if the system described by the Hamiltonian $H_A(t)$ has a non-zero energy gap between the ground state and the excited states, and has a unique ground state, then the ground state of H is obtained by the time evolution

$$|\text{vac}\rangle = \lim_{T \rightarrow \infty} \mathcal{T} \exp \left(-i \int_0^T dt H_A(t) \right) |\text{vac}\rangle_0. \quad (17)$$

In practice, we take finite T and discretize the integral, and therefore we can obtain only an approximation of the vacuum. This implies that an expectation value of an operator under the approximate vacuum has intrinsic

⁴ If we took a periodic boundary condition, then L_0 was dynamical and one of ϕ_n 's could not be eliminated by the redefinition.

systematic errors. In Appendix D, we discuss how we estimate the systematic errors.

In our quantum simulation, we take the initial Hamiltonian H_0 as

$$H_0 = H_{ZZ} + H_Z|_{m \rightarrow m_0, \theta \rightarrow 0}, \quad (18)$$

where $m_0 \in \mathbb{R}_{\geq 0}$ can be arbitrary in principle, however, is chosen so that the estimated systematic errors become small. The ground state of H_0 is

$$|\text{vac}\rangle_0 = |0\rangle \otimes |1\rangle \otimes \cdots \otimes |0\rangle \otimes |1\rangle, \quad (19)$$

where $Z|0\rangle = |0\rangle$ and $Z|1\rangle = -|1\rangle$. In order to evolve it into the desired vacuum state we choose the following adiabatic Hamiltonian,

$$H_A(t) = H_{ZZ} + H_{\pm, A}(t) + H_{Z, A}(t), \quad (20)$$

with $H_{\pm, A}$ and $H_{Z, A}$ obtained by replacing the parameters of H_{\pm} and H_Z in the Hamiltonian (11) as

$$w \rightarrow \frac{t}{T}w, \quad \theta \rightarrow \frac{t}{T}\theta, \quad m \rightarrow \left(1 - \frac{t}{T}\right)m_0 + \frac{t}{T}m. \quad (21)$$

We take finite T and approximate the time evolution (17) by

$$|\text{vac}\rangle \simeq U(T)U(T - \delta t) \cdots U(2\delta t)U(\delta t)|\text{vac}\rangle_0, \quad (22)$$

where $U(t) = e^{-iH_A(t)\delta t}$ and $\delta t = \frac{T}{M}$ with a large positive integer M . The most naive way to approximate the operator $U(t)$ is

$$U(t) = e^{-iH_{ZZ}\delta t} e^{-iH_{\pm, A}(t)\delta t} e^{-iH_{Z, A}(t)\delta t} + \mathcal{O}(\delta t^2). \quad (23)$$

While we use this approximation for $\theta = 0$ with $(T, \delta t) = (100, 0.1)$, we use an improved version of (23), with $\mathcal{O}(\delta t^3)$ error, for $\theta \neq 0$ with $(T, \delta t) = (150, 0.3)$ which is discussed in Appendix E. We implement all the operators in the time evolution by combinations of quantum elementary gates provided by IBM Qiskit library (see Appendix C). Finally, in the process of measuring the mass operator, we take the number of shots to be 10^6 in all the data points. This induces statistical errors in addition to the systematic errors.

IV. RESULTS

A. Massless case

Let us first focus on the massless case and compare with the exact result in the continuum theory [14–17],

$$\langle \bar{\psi}(x)\psi(x) \rangle = -\frac{e^\gamma}{2\pi^{3/2}}g \approx -0.160g, \quad (24)$$

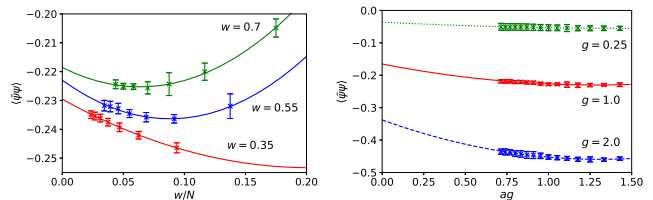


FIG. 1: [Left] Infinite volume limits for some values of w at $g = 1$, $m = 0$, $\theta = 0$. For each w , we compute the chiral condensation for $N = [4, 16]$ and extrapolate it to $N \rightarrow \infty$ by fitting the data by quadratic polynomial of w/N . The error bars in the data points include both statistical and systematic errors. [Right] Continuum limits at $m = 0, \theta = 0$ for some values of g . The curves show fitting functions by quadratic functions of ag . The error bars are fitting errors in taking the infinite volume limit.

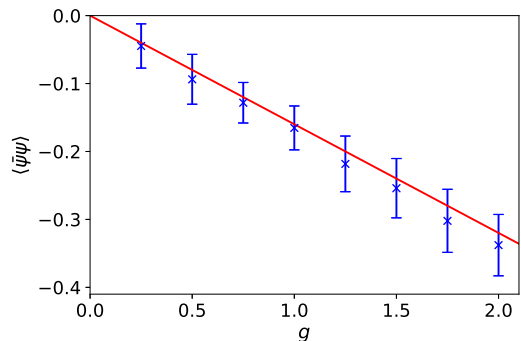


FIG. 2: The VEV of the mass operator for $m = 0$ is plotted against coupling constant g . The red solid line shows the exact result, which is approximately $-0.160g$. The error bars are fitting errors of the continuum limit.

where γ is the Euler-Mascheroni constant. Note that the θ -parameter is irrelevant in this case since our lattice Hamiltonian is independent of θ for $m = 0$. We take a continuum limit for fixed physical parameters (g, m, θ) in two steps: (i) Take infinite volume limit. Namely, for fixed $w = 1/2a$ and the physical parameters, we compute the observables for various N 's and then extrapolate them to $N \rightarrow \infty$. Repeating this for multiple values of w , we obtain data of infinite volume limit for various lattice spacing a at fixed physical parameters. This step is illustrated in fig. 1 [Left]. (ii) Extrapolate the data of the infinite volume limit to the continuum limit $a \rightarrow 0$. This procedure is demonstrated in fig. 1 [Right].

Repeating the above procedures, we have obtained g dependence of the mass operator in the continuum limit as shown in fig. 2. We see that our result agrees with the exact result. Note that the massless case cannot be easily explored by the standard Monte Carlo approach because

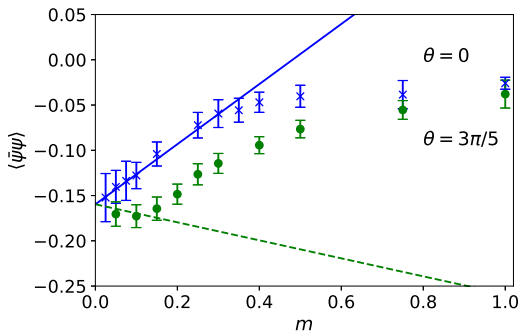


FIG. 3: The VEV of the mass operator at $g = 1$ is plotted against the mass m for $\theta = 0$ (blue \times 's) and $\theta = 3\pi/5$ (green circles). The lines show the result (25) of the mass perturbation. The error bars are fitting errors in taking the continuum limit.

computational cost to evaluate effects of fermions in the standard approach is $O((am)^{-1})$ [64]. This point is another advantage of our approach over the standard Monte Carlo approach.

B. Massive case

Next, we consider the massive case. For this case, there is a result by mass perturbation theory [18, 19]:

$$\langle \bar{\psi}(x)\psi(x) \rangle \approx -0.160g + 0.322m \cos \theta, \quad (25)$$

up to $\mathcal{O}(m^2)$. There is a subtlety in comparison with this result: the observable is UV divergent logarithmically and we need to regularize it. Here we adopt a lattice counterpart of a regularization used in [18] which is a subtraction of the free theory result. Specifically, for a given lattice spacing a , we take infinite volume limit without subtraction as in fig. 1 [Left] but subtract the result at $J = 0$ and $N \rightarrow \infty$ in taking the continuum limit:

$$\begin{aligned} \langle \bar{\psi}(x)\psi(x) \rangle_{\text{free}} = & -\frac{m \cos \theta}{\pi \sqrt{1 + (ma \cos \theta)^2}} \\ & \times \int_0^{\pi/2} \frac{dt}{\sqrt{1 - \frac{1 - (ma \sin \theta)^2}{1 + (ma \cos \theta)^2} \sin^2 t}}. \end{aligned} \quad (26)$$

In other words, we replace $\langle \bar{\psi}\psi \rangle$ in fig. 1 [Right] by $\langle \bar{\psi}\psi \rangle - \langle \bar{\psi}\psi \rangle_{\text{free}}$ for the massive case.

In fig. 3, we plot our result in the continuum limit for $(g, \theta) = (1, 0)$ and $(g, \theta) = (1, 3\pi/5)$ against m , and compare with the mass perturbation theory (25). We see that our result agrees with the mass perturbation theory in small mass regime for the both values of θ . As increasing mass, it deviates from (25) and finally approaches

zero. This large mass asymptotic behavior is expected since the large mass limit should be the same as the free theory result which we have subtracted. Our result for $\theta = 0$ also agrees with previous numerical result obtained by tensor network approach [65]. Thus we conclude that our approach practically works well for nonzero (g, m, θ) .

V. SUMMARY AND DISCUSSIONS

In this letter, we have implemented the digital quantum simulation of the Schwinger model with the θ -term as the first example of digital quantum simulation of gauge theory with topological terms. We have converted the Schwinger model to the spin system on the spatial lattice and then constructed the true vacuum state of the model using adiabatic state preparation. We have computed VEV of the fermion mass operator, taken the continuum limit and found agreement with the results in literature. Our results imply that digital quantum simulation is already useful tool to explore non-perturbative aspects of gauge theories with real time and topological terms.

Here we have used the quantum simulator to see how our algorithm practically works and grasp a future prospect on applications of real quantum computers to quantum field theory. The maximal number of qubits in our simulation is 16, which is not so big even in current technology. While this is quite encouraging, the adiabatic preparation of state adopted here requires a large number of gates: our quantum circuit for 16 qubits without improvement of Trotter decomposition has about 250 single-qubit gates and 270 two-qubit gates at each time step which has been repeated about 1000 times. This would need much more hardware resources and future developments in implementing our simulation in real quantum computers. Therefore it is important to save the number of gates by improving the algorithm. We have demonstrated that one could take three times coarser time steps δT by using the second-order decomposition which reduces the total number of gates by 40% compared to the unimproved decomposition to achieve similar size of errors in appendix E. One could also change the adiabatic Hamiltonian (20) so that we can take smaller adiabatic time T . In principle, the adiabatic Hamiltonian $H_A(t)$ can be any hermitian operator satisfying (16) as long as the system during the adiabatic process has a energy gap and has a unique ground state.

There are various interesting applications and generalization of our work. An obvious application is to compute other observables in the Schwinger model. Specifically, the massive Schwinger model is known to exhibit confinement [66] and therefore it would be interesting

to explore physics of confinement in a situation where standard Monte Carlo approach is inapplicable. Another interesting direction is to apply our methods to other theories. The formulation to rewrite gauge theory in terms of qubits can be directly applied to any $1+1$ dimensional $U(1)$ gauge theory coupled to fermions. It would also be interesting to implement a digital quantum simulation of $1+1$ dimensional non-Abelian gauge theories.

Acknowledgement

The results of this work have been obtained by using quantum simulator in IBM Qiskit library. Y.K. would like to thank Dmitri E. Kharzeev for discussions on closely related projects. B.C. and M.H. have been partially supported by STFC consolidated grant ST/P000681/1. The work of A.T. was supported by the RIKEN Special Postdoctoral Researcher program. T.I. is supported in part by US DOE Contract DESC0012704(BNL). T.I. is also supported by JSPS KAKENHI grant number JP17H02906.

Appendix A: Operator correspondence between Dirac and Staggered fermions

The Dirac fermion operator $\psi(x) = (\psi_u(x), \psi_d(x))^\top$ is translated into those of staggered fermions as follows [61, 62],

$$\frac{\chi_n}{\sqrt{a}} \leftrightarrow \begin{cases} \psi_u(x) & n : \text{even} \\ \psi_d(x) & n : \text{odd} \end{cases}. \quad (\text{A1})$$

Here, we see how the bilinear operators $\bar{\psi}\gamma^1\partial_1\psi$, $\bar{\psi}\psi$, and $\bar{\psi}\gamma^5\psi$ are written in terms of the staggered fermions. We start with the fermion kinetic operator $\bar{\psi}\gamma^1\partial_1\psi$:

$$\begin{aligned} & \bar{\psi}(x)\gamma^1\partial_1\psi(x) \\ &= \psi_u^\dagger(x) \frac{\psi_d(x+1) - \psi_d(x)}{2a} + \psi_d^\dagger(x) \frac{\psi_u(x) - \psi_u(x-1)}{2a}, \\ &= \frac{1}{2a^2} \left[\chi_{2x}^\dagger(\chi_{2x+1} - \chi_{2x-1}) + \chi_{2x-1}^\dagger(\chi_{2x} - \chi_{2x-2}) \right]. \end{aligned} \quad (\text{A2})$$

Thus, we arrive at the following expression,

$$a \sum_{x=1}^{N/2} \bar{\psi}(x)\gamma^1\partial_1\psi(x) = \frac{1}{2a} \sum_{n=1}^N [\chi_n^\dagger\chi_{n+1} - \chi_{n+1}^\dagger\chi_n]. \quad (\text{A3})$$

Next, we convert the fermion mass operator $\bar{\psi}\psi$:

$$\begin{aligned} \bar{\psi}(x)\psi(x) &= \psi_u^\dagger(x)\psi_u(x) - \psi_d^\dagger(x)\psi_d(x), \\ &= \frac{1}{a} \left[\chi_{2x}^\dagger\chi_{2x} - \chi_{2x-1}^\dagger\chi_{2x-1} \right], \end{aligned} \quad (\text{A4})$$

which leads us to

$$a \sum_{x=1}^{N/2} \bar{\psi}(x)\psi(x) = \sum_{n=1}^N (-1)^n \chi_n^\dagger\chi_n. \quad (\text{A5})$$

Finally, we consider the pseudo mass operator $\bar{\psi}\gamma_5\psi$. Since it is a fermion bilinear operator involving off-diagonal matrix, the conversion to staggered fermion yields hopping term connecting even and odd sites:

$$\begin{aligned} \bar{\psi}(x)\gamma_5\psi(x) &= \psi_u^\dagger(x)\psi_d(x) - \psi_d^\dagger(x)\psi_u(x) \\ &\approx \frac{1}{2} \left[\psi_u^\dagger(x)\psi_d(x) - \psi_d^\dagger(x)\psi_u(x) \right] \\ &+ \frac{1}{2} \left[\psi_u^\dagger(x)\psi_d(x+1) - \psi_d^\dagger(x+1)\psi_u(x) \right] \\ &= -\frac{1}{2a} \left[\chi_{2x-1}^\dagger\chi_{2x} - \chi_{2x}^\dagger\chi_{2x-1} \right] \\ &+ \frac{1}{2a} \left[\chi_{2x}^\dagger\chi_{2x+1} - \chi_{2x+1}^\dagger\chi_{2x} \right], \end{aligned} \quad (\text{A6})$$

where we have used $\psi_d(x+1) = \psi_d(x) + \mathcal{O}(a)$ to modify the operator, that recovers the original one in the continuum limit $a \rightarrow 0$. Thus the pseudo mass operator is

rewritten as

$$\sum_{x=1}^{N/2} \bar{\psi}(x)\gamma_5\psi(x) = \frac{1}{2} \sum_{n=1}^N (-1)^n \left[\chi_n^\dagger\chi_{n+1} - \chi_{n+1}^\dagger\chi_n \right]. \quad (\text{A7})$$

Appendix B: Alternative method: without chiral rotation

Here we rewrite the Schwinger model based on the Lagrangian (1) without the chiral rotation in terms of the spin variables. In the temporal gauge, conjugate momentum of A^1 is

$$\Pi = \frac{\partial \mathcal{L}}{\partial \dot{A}^1} = \dot{A}^1 + \frac{g\theta}{2\pi}, \quad (\text{B1})$$

and therefore the Hamiltonian is

$$H = \int dx \left[-i\bar{\psi}\gamma^1(\partial_1 + igA_1)\psi + m\bar{\psi}\psi + \frac{1}{2} \left(\Pi - \frac{g\theta}{2\pi} \right)^2 \right]. \quad (\text{B2})$$

Using the staggered fermion, the lattice Hamiltonian is given by

$$\begin{aligned} H &= -iw \sum_{n=1}^{N-1} \left[\chi_n^\dagger e^{i\phi_n} \psi_{n+1} - \chi_{n+1}^\dagger e^{-i\phi_n} \chi_n \right] \\ &+ m \sum_{n=1}^N (-1)^n \chi_n^\dagger\chi_n + J \sum_{n=1}^{N-1} \left(L_n + \frac{\theta}{2\pi} \right)^2, \end{aligned} \quad (\text{B3})$$

where L_n corresponds to $-\Pi(x)/g$ and the operators satisfy the commutation relations (7) as well as the Gauss law (8) on physical states. Applying the Jordan-Wigner transformation (9), taking the open boundary condition with constant L_0 and solving the Gauss law, we obtain the lattice Hamiltonian

$$\begin{aligned} H &= w \sum_{n=1}^{N-1} \left[\sigma_n^+ \sigma_{n+1}^- + \text{h.c.} \right] + \frac{m}{2} \sum_{n=1}^N (-1)^n Z_n \\ &+ J \sum_{n=1}^{N-1} \left[L_0 + \frac{\theta}{2\pi} + \frac{1}{2} \sum_{\ell=1}^n (Z_\ell + (-1)^\ell) \right]^2. \end{aligned} \quad (\text{B4})$$

In this formulation, it is clear that the theory with (θ, L_0) is equivalent to $(\theta + 2\pi L_0, 0)$. Digital quantum simulation in this formulation can be implemented in a similar way to the formulation in the main text. It would be interesting to perform a digital quantum simulation in this formulation and see how this formulation practically works.

Appendix C: Details on quantum simulation protocol

Here we write down all the qubit operations used in quantum circuits in this paper. First we write down single qubit operation which acts on a superposition of

$$|0\rangle = \begin{pmatrix} 1 \\ 0 \end{pmatrix} \quad \text{and} \quad |1\rangle = \begin{pmatrix} 0 \\ 1 \end{pmatrix}. \quad (\text{C1})$$

Some of most basic operations are Pauli matrices:

$$X = \begin{pmatrix} 0 & 1 \\ 1 & 0 \end{pmatrix}, \quad Y = \begin{pmatrix} 0 & -i \\ i & 0 \end{pmatrix}, \quad Z = \begin{pmatrix} 1 & 0 \\ 0 & -1 \end{pmatrix} \quad (\text{C2})$$

In terms of (X, Y, Z) , we also use

$$R_X(\phi) = e^{-\frac{i\phi}{2}X}, \quad R_Y(\phi) = e^{-\frac{i\phi}{2}Y}, \quad R_Z(\phi) = e^{-\frac{i\phi}{2}Z}. \quad (\text{C3})$$

The only two qubit operation used in this paper is controlled- X (controlled-NOT):

$$CX = \begin{pmatrix} 1 & 0 & 0 & 0 \\ 0 & 1 & 0 & 0 \\ 0 & 0 & 0 & 1 \\ 0 & 0 & 1 & 0 \end{pmatrix} = \begin{array}{c} \text{---} \bullet \text{---} \\ | \\ \text{---} \oplus \text{---} \end{array} \quad (\text{C4})$$

which acts on superposition of $|i\rangle \otimes |j\rangle$ with $i, j = 0, 1$. In particular, CX satisfies

$$CX|0\rangle \otimes |\alpha\rangle = |0\rangle \otimes |\alpha\rangle, \quad CX|1\rangle \otimes |\alpha\rangle = |1\rangle \otimes X|\alpha\rangle. \quad (\text{C5})$$

We can construct all the operators in (23) by combinations of the quantum elementary gates $R_{X,Y,Z}$ and CX . First, $e^{-iH_Z\delta t}$ is simply realized by a product of single qubit operations:

$$e^{-iH_Z\delta t} = \prod_{n=1}^N R_Z^{(n)}(2c_n\delta t), \quad (\text{C6})$$

where $R_Z^{(n)}(\phi)$ stands for a $R_Z(\phi)$ gate acting on n -th qubit and c_n is defined by $\sum_{n=1}^N c_n Z_n = H_{Z,A}(t)$. The other two unitary operators in (23) involve two-qubit operations. The operator $e^{-iH_{ZZ}\delta t}$ needs the following two-qubit operations of

$$e^{-i\frac{J\delta t}{2}Z_1Z_2}, \quad (\text{C7})$$

to appropriate pairs of qubits. This operator is the same as the interaction of the Ising model and its concrete realization is,

$$e^{-i\frac{J\delta t}{2}Z_1Z_2} = CX^{(12)}R_Z^{(2)}(J\delta t)CX^{(12)}, \quad (\text{C8})$$

with a quantum gate given by

$$e^{-i\frac{J\delta t}{2}Z_1Z_2} = \begin{array}{c} \text{---} \boxed{Z_1Z_2(\frac{J\delta t}{2})} \text{---} \\ | \\ \text{---} \bullet \text{---} \\ | \\ \text{---} \oplus \text{---} \end{array} \quad (\text{C9})$$

The operator $e^{-iH_{\pm}\frac{t\delta t}{T}}$ can be constructed in a similar way. It needs the two qubit operations of

$$e^{-i\frac{\tilde{w}\delta t}{2}(X_1X_2+Y_1Y_2)} = e^{-i\frac{\tilde{w}\delta t}{2}X_1X_2}e^{-i\frac{\tilde{w}\delta t}{2}Y_1Y_2} + \mathcal{O}(\delta t^2), \quad (\text{C10})$$

to appropriate pairs. Here, \tilde{w} is defined by $\tilde{w} := \frac{t}{T}w - \frac{(-1)^n}{2}((1 - \frac{t}{T})m_0 + m)\sin(\theta\frac{t}{T})$. This is concretely realized by

$$e^{-i\frac{\tilde{w}\delta t}{2}X_1X_2} = CX^{(12)}R_X^{(1)}(\tilde{w}\delta t)CX^{(12)}, \quad (\text{C11})$$

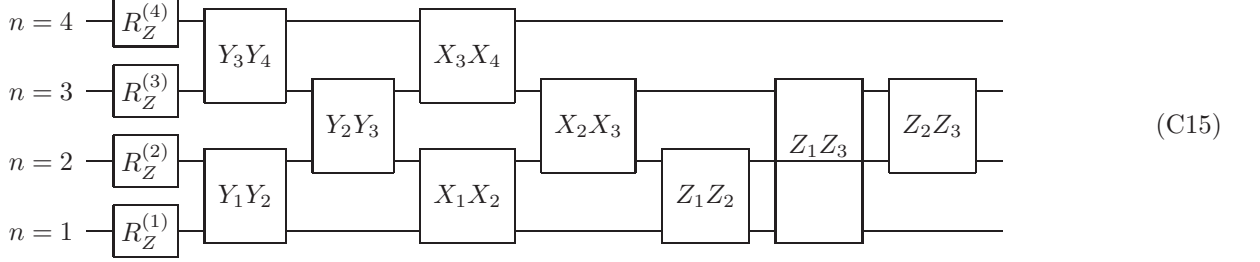
$$e^{-i\frac{\tilde{w}\delta t}{2}Y_1Y_2} = \prod_{j=1}^2 R_Z^{(j)}\left(\frac{\pi}{2}\right) \cdot e^{-i\frac{\tilde{w}\delta t}{2}X_1X_2} \cdot \prod_{j=1}^2 R_Z^{(j)}\left(-\frac{\pi}{2}\right), \quad (\text{C12})$$

whose circuit diagrams are respectively given by

$$e^{-i\frac{\tilde{w}\delta t}{2}X_1X_2} = \begin{array}{c} \text{---} \boxed{X_1X_2(\frac{\tilde{w}\delta t}{2})} \text{---} \\ | \\ \text{---} \bullet \text{---} \\ | \\ \text{---} \oplus \text{---} \end{array} \quad (\text{C13})$$

$$e^{-i\frac{\tilde{w}\delta t}{2}Y_1Y_2} = \begin{array}{c} \text{---} \boxed{Y_1Y_2(\frac{\tilde{w}\delta t}{2})} \text{---} \\ | \\ \text{---} \boxed{R_Z(-\frac{\pi}{2})} \text{---} \boxed{X_1X_2(\frac{\tilde{w}\delta t}{2})} \boxed{R_Z(\frac{\pi}{2})} \text{---} \\ | \\ \text{---} \boxed{R_Z(-\frac{\pi}{2})} \text{---} \boxed{X_1X_2(\frac{\tilde{w}\delta t}{2})} \boxed{R_Z(\frac{\pi}{2})} \text{---} \end{array} \quad (\text{C14})$$

For example, we implement the time evolution operator $U(t)$ (23) with lattice size $N = 4$ by the following quantum circuit:



(C15)

where the argument of each unitary gate is suppressed and can be read off from (12), (21), and (23): $R_Z^{(n)} \rightarrow R_Z^{(n)}(2c_n \delta t)$, $X_n X_{n+1} \rightarrow X_n X_{n+1}(\frac{\tilde{w} \delta t}{2})$, $Y_n Y_{n+1} \rightarrow Y_n Y_{n+1}(\frac{\tilde{w} \delta t}{2})$, $Z_1 Z_2 \rightarrow Z_1 Z_2(J \delta t)$, $Z_1 Z_3 \rightarrow Z_1 Z_3(\frac{J \delta t}{2})$ and $Z_2 Z_3 \rightarrow Z_2 Z_3(\frac{J \delta t}{2})$.

Appendix D: Estimation of systematic errors

Here we explain how we estimate systematic errors due to the approximations in the adiabatic process shown in the main text. A VEV of an operator \mathcal{O} is defined by

$$\langle \mathcal{O} \rangle = \langle 0 | \mathcal{O} | 0 \rangle, \quad (\text{D1})$$

where in this appendix we denote ground state of a system under consideration by $|0\rangle$. Suppose we would like to find an approximation of this quantity by using an adiabatic preparation of the vacuum as in the main text. Let us denote the approximate vacuum obtained in this way as $|0_A\rangle$. Then we approximate the VEV (D1) by

$$\langle \mathcal{O} \rangle_A = \langle 0_A | \mathcal{O} | 0_A \rangle, \quad (\text{D2})$$

which is generically different from the true VEV. The state $|0_A\rangle$ can be expanded as

$$|0_A\rangle = \sum_{n=0}^{\infty} c_n |n\rangle, \quad (\text{D3})$$

where $|n\rangle$ is the n -th excited state of the full Hamiltonian H of the system. If we take the adiabatic time T and the number of steps M in the Suzuki-Trotter decomposition sufficiently large, then we expect $|c_0| \simeq 1 \gg |c_{n \neq 0}|$ and $|0_A\rangle$ is almost the true vacuum.

Now we propose how to estimate systematic error in approximating the VEV (D1) by (D2). Let us consider the quantity

$$\langle \mathcal{O} \rangle_A(t) = \langle 0_A | e^{iHt} \mathcal{O} e^{-iHt} | 0_A \rangle. \quad (\text{D4})$$

If we managed to prepare the vacuum exactly i.e. $|0_A\rangle = |0\rangle$, then this quantity was reduced to $\langle \mathcal{O} \rangle$ and independent of t since the vacuum is the eigenstate of H . However, this quantity depends on t when we have only approximation of the vacuum. Let us see how it depends on t using the expansion (D3):

where the argument of each unitary gate is suppressed and can be read off from (12), (21), and (23): $R_Z^{(n)} \rightarrow R_Z^{(n)}(2c_n \delta t)$, $X_n X_{n+1} \rightarrow X_n X_{n+1}(\frac{\tilde{w} \delta t}{2})$, $Y_n Y_{n+1} \rightarrow Y_n Y_{n+1}(\frac{\tilde{w} \delta t}{2})$, $Z_1 Z_2 \rightarrow Z_1 Z_2(J \delta t)$, $Z_1 Z_3 \rightarrow Z_1 Z_3(\frac{J \delta t}{2})$ and $Z_2 Z_3 \rightarrow Z_2 Z_3(\frac{J \delta t}{2})$.

$$\begin{aligned} \langle \mathcal{O} \rangle_A(t) &= \sum_{n=0}^{\infty} |c_n|^2 \langle n | \mathcal{O} | n \rangle \\ &+ 2 \sum_{m \neq n} \text{Re} \left(c_m^* c_n e^{i(E_m - E_n)t} \langle m | \mathcal{O} | n \rangle \right), \end{aligned} \quad (\text{D5})$$

which implies that this quantity oscillates around the constant $\sum_{n=0}^{\infty} |c_n|^2 \langle n | \mathcal{O} | n \rangle$ as varying t . If we have a good approximation of the vacuum s.t. $|c_0| \gg |c_{n \neq 0}|$, then we approximately have

$$\begin{aligned} \langle \mathcal{O} \rangle_A(t) &\simeq |c_0|^2 \left[\langle \mathcal{O} \rangle + \sum_{n=1}^{\infty} \text{Re} \left(\frac{2c_n^* c_0}{|c_0|^2} e^{i(E_n - E_0)t} \langle n | \mathcal{O} | 0 \rangle \right) \right. \\ &\left. + \mathcal{O} \left(\left| \frac{c_n}{c_0} \right|^2 \right) \right], \end{aligned} \quad (\text{D6})$$

which approximately oscillates around $\simeq \langle \mathcal{O} \rangle$, and the amplitude of the oscillation read from the quantity $\langle \mathcal{O} \rangle_A(t)$ represents intrinsic errors in predicting the true VEV $\langle \mathcal{O} \rangle$ by the adiabatic state preparation. Thus, in the main text, we estimate

$$\frac{1}{2} (\max \langle \mathcal{O} \rangle_A(t) + \min \langle \mathcal{O} \rangle_A(t)) \quad (\text{D7})$$

as central value, and

$$\frac{1}{2} (\max \langle \mathcal{O} \rangle_A(t) - \min \langle \mathcal{O} \rangle_A(t)) \quad (\text{D8})$$

as systematic error in approximating the true VEV $\langle \mathcal{O} \rangle$ by the adiabatic preparation of the vacuum.

Fig. 4 demonstrates the above procedure for the VEV of the mass operator computed in the main text. In fig. 4 [Left], we fix the Trotter step to $\delta t = 0.1$ and plot the results for different values of the adiabatic time T . We find that the expectation value of the mass operator under the state $e^{-iHt} |0_A\rangle$ oscillates around the true VEV obtained of the Hamiltonian as expected. We also find

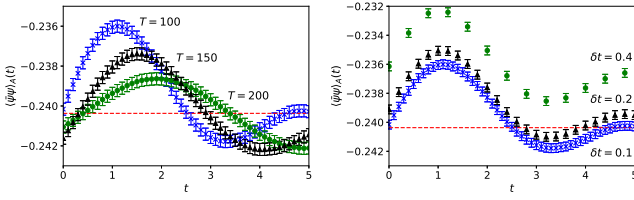


FIG. 4: The expectation value of the mass operator under the state $e^{-iHt}|0_A\rangle$ for $(g, m, N, w) = (1, 0, 4, 0.5)$ against t obtained by simulations with $m_0 = 0.5$ and 10^6 shots. The red dashed line is the result obtained by diagonalization of the Hamiltonian. The error bars are statistical errors. [Left] At fixed $\delta t = 0.1$ with some values of T [Right] At fixed $T = 100$ with some values of δt

that the result with larger T has smaller amplitude. This reflects the fact that the approximate vacuum $|0_A\rangle$ with larger T is closer to the true vacuum and therefore the systematic error must be smaller for larger T . In fig. 4 [Right], we fix T as $T = 100$ and plot the results for different values of δt . The green circles show that if we do not take sufficiently small δt , then approximation of the time evolution operator e^{-iHt} breaks down and it does not oscillates around the correct value. Thus, it is important to take appropriate values of T and δt to get reasonable approximations.

Appendix E: Improvement of the Suzuki-Trotter decomposition

The first-order Suzuki-Trotter decomposition is

$$e^{-i(H_1+H_2)\delta t} = e^{-iH_1\delta t}e^{-iH_2\delta t} + \mathcal{O}(\delta t^2), \quad (\text{E1})$$

for non-commuting operators H_1 and H_2 . This error is reduced by using the second-order decomposition,

$$e^{-i(H_1+H_2)\delta t} = e^{-iH_1\frac{\delta t}{2}}e^{-iH_2\delta t}e^{-iH_1\frac{\delta t}{2}} + \mathcal{O}(\delta t^3). \quad (\text{E2})$$

Let us apply this improvement to our adiabatic state preparation. First we decompose the adiabatic Hamiltonian as

$$H_A(t) = \tilde{H}_Z(t) + \tilde{H}_X(t) + \tilde{H}_Y(t), \quad (\text{E3})$$

where

$$\tilde{H}_Z = H_{ZZ} + H_{Z,A}(t)$$

$$\tilde{H}_X = \frac{1}{2} \sum_{n=1}^{N-1} h_{XY}(t) X_n X_{n+1},$$

$$\tilde{H}_Y = \frac{1}{2} \sum_{n=1}^{N-1} h_{XY}(t) Y_n Y_{n+1},$$

$$h_{XY}(t) = \frac{t}{T} w - \frac{(-1)^n}{2} \left[\left(1 - \frac{t}{T}\right) m_0 + \frac{t}{T} m \right] \sin\left(\frac{t}{T}\theta\right). \quad (\text{E4})$$

This implies that the Hamiltonian can be divided into three sets of operators:

$$\begin{aligned} \tilde{H}_Z &: \{Z_1, \dots, Z_N, Z_1 Z_2, Z_1 Z_3, \dots, Z_{N-1} Z_N\}, \\ \tilde{H}_X &: \{X_1 X_2, X_2 X_3, \dots, X_{N-1} X_N\}, \\ \tilde{H}_Y &: \{Y_1 Y_2, Y_2 Y_3, \dots, Y_{N-1} Y_N\}. \end{aligned} \quad (\text{E5})$$

The operators commute with each other within each set. Then the time evolution operator $U(t) = e^{-iH_A(t)\delta t}$ is approximated by

$$U(t) = e^{-i\tilde{H}_Y\frac{\delta t}{2}}e^{-i\tilde{H}_X\frac{\delta t}{2}}e^{-i\tilde{H}_Z\delta t}e^{-i\tilde{H}_X\frac{\delta t}{2}}e^{-i\tilde{H}_Y\frac{\delta t}{2}} + \mathcal{O}(\delta t^3). \quad (\text{E6})$$

In this improvement, the quantum circuit for 16 qubits has about 400 single-qubit gates and 500 two-qubit gates at each time step while the one without the improvement has 250 single-qubit gates and 270 two-qubit gates. Note that the improvement saves the number of gates in the total time evolution since it needs smaller time steps to achieve the same accuracy.

-
- [1] C. Ratti, “Lattice QCD and heavy ion collisions: a review of recent progress,” *Rept. Prog. Phys.* **81** no. 8, (2018) 084301, [arXiv:1804.07810 \[hep-lat\]](#).
- [2] H.-W. Lin, “Review of Baryon Spectroscopy in Lattice QCD,” *Chin. J. Phys.* **49** (2011) 827, [arXiv:1106.1608 \[hep-lat\]](#).
- [3] O. Philipsen, “The QCD equation of state from the lattice,” *Prog. Part. Nucl. Phys.* **70** (2013) 55–107, [arXiv:1207.5999 \[hep-lat\]](#).
- [4] H.-T. Ding, F. Karsch, and S. Mukherjee, “Thermodynamics of strong-interaction matter from

Lattice QCD,”

Int. J. Mod. Phys. **E24** no. 10, (2015) 1530007, [arXiv:1504.05274 \[hep-lat\]](#).

- [5] T. Izubuchi, S. Aoki, K. Hashimoto, Y. Nakamura, T. Sekido, and G. Schierholz, “Dynamical QCD simulation with theta terms,” *PoS LATTICE2007* (2007) 106, [arXiv:0802.1470 \[hep-lat\]](#).
- [6] G. Aarts, “Introductory lectures on lattice QCD at nonzero baryon number,” *J. Phys. Conf. Ser.* **706** no. 2, (2016) 022004, [arXiv:1512.05145 \[hep-lat\]](#).

- [7] S. Takeda, “Tensor network approach to real-time path integral,” in *37th International Symposium on Lattice Field Theory (Lattice 2019) Wuhan, Hubei, China, June 16-22, 2019*. 2019. [arXiv:1908.00126 \[hep-lat\]](#).
- [8] J. Preskill, “Quantum computing and the entanglement frontier,” [arXiv:1203.5813 \[quant-ph\]](#).
- [9] F. Arute *et al.*, “Quantum supremacy using a programmable superconducting processor,” *Nature* **574** no. 7779, (2019) 505–510.
- [10] J. S. Schwinger, “Gauge Invariance and Mass,” *Phys. Rev.* **125** (1962) 397–398. [,151(1962)].
- [11] S. R. Coleman, R. Jackiw, and L. Susskind, “Charge Shielding and Quark Confinement in the Massive Schwinger Model,” *Annals Phys.* **93** (1975) 267.
- [12] S. R. Coleman, “More About the Massive Schwinger Model,” *Annals Phys.* **101** (1976) 239.
- [13] N. S. Manton, “The Schwinger Model and Its Axial Anomaly,” *Annals Phys.* **159** (1985) 220–251.
- [14] J. E. Hetrick and Y. Hosotani, “QED ON A CIRCLE,” *Phys. Rev.* **D38** (1988) 2621.
- [15] J. E. Hetrick, Y. Hosotani, and S. Iso, “The Massive multi - flavor Schwinger model,” *Phys. Lett.* **B350** (1995) 92–102, [arXiv:hep-th/9502113 \[hep-th\]](#).
- [16] Y. Hosotani, R. Rodriguez, J. E. Hetrick, and S. Iso, “Confinement and chiral dynamics in the multiflavor Schwinger model,” in *Continuous advances in QCD 1996. Proceedings, Conference, Minneapolis, USA, March 28-31, 1996*, pp. 382–390. 1996. [arXiv:hep-th/9606129 \[hep-th\]](#).
- [17] Y. Hosotani, “Gauge theory model: Quark dynamics and antiferromagnets,” in *Physics. Proceedings, 2nd International A.D. Sakharov Conference, Moscow, Russia, May 20-24, 1996*, pp. 445–449. 1996. [arXiv:hep-th/9606167 \[hep-th\]](#).
- [18] C. Adam, “Normalization of the chiral condensate in the massive Schwinger model,” *Phys. Lett.* **B440** (1998) 117–122, [arXiv:hep-th/9806211 \[hep-th\]](#).
- [19] C. Adam, “Massive Schwinger model within mass perturbation theory,” *Annals Phys.* **259** (1997) 1–63, [arXiv:hep-th/9704064 \[hep-th\]](#).
- [20] J. Preskill, “Quantum Computing in the NISQ era and beyond,” *Quantum* **2** (Aug., 2018) 79. <https://doi.org/10.22331/q-2018-08-06-79>.
- [21] S. P. Jordan, K. S. M. Lee, and J. Preskill, “Quantum Algorithms for Quantum Field Theories,” *Science* **336** (2012) 1130–1133, [arXiv:1111.3633 \[quant-ph\]](#).
- [22] S. P. Jordan, K. S. M. Lee, and J. Preskill, “Quantum Computation of Scattering in Scalar Quantum Field Theories,” [arXiv:1112.4833 \[hep-th\]](#). [Quant. Inf. Comput.14,1014(2014)].
- [23] S. P. Jordan, K. S. M. Lee, and J. Preskill, “Quantum Algorithms for Fermionic Quantum Field Theories,” [arXiv:1404.7115 \[hep-th\]](#).
- [24] L. Garc C -a C lvarez, J. Casanova, A. Mezzacapo, I. L. Egusquiza, L. Lamata, G. Romero, and E. Solano, “Fermion-Fermion Scattering in Quantum Field Theory with Superconducting Circuits,” *Phys. Rev. Lett.* **114** no. 7, (2015) 070502, [arXiv:1404.2868 \[quant-ph\]](#).
- [25] U.-J. Wiese, “Towards Quantum Simulating QCD,” *Nucl. Phys.* **A931** (2014) 246–256, [arXiv:1409.7414 \[hep-th\]](#).
- [26] D. Marcos, P. Widmer, E. Rico, M. Hafezi, P. Rabl, U. J. Wiese, and P. Zoller, “Two-dimensional Lattice Gauge Theories with Superconducting Quantum Circuits,” *Annals Phys.* **351** (2014) 634–654, [arXiv:1407.6066 \[quant-ph\]](#).
- [27] A. Mezzacapo, E. Rico, C. Sab C -n, I. L. Egusquiza, L. Lamata, and E. Solano, “Non-Abelian $SU(2)$ Lattice Gauge Theories in Superconducting Circuits,” *Phys. Rev. Lett.* **115** no. 24, (2015) 240502, [arXiv:1505.04720 \[quant-ph\]](#).
- [28] E. A. Martinez *et al.*, “Real-time dynamics of lattice gauge theories with a few-qubit quantum computer,” *Nature* **534** (2016) 516–519, [arXiv:1605.04570 \[quant-ph\]](#).
- [29] C. Muschik, M. Heyl, E. Martinez, T. Monz, P. Schindler, B. Vogell, M. Dalmonte, P. Hauke, R. Blatt, and P. Zoller, “ $U(1)$ Wilson lattice gauge theories in digital quantum simulators,” *New J. Phys.* **19** no. 10, (2017) 103020, [arXiv:1612.08653 \[quant-ph\]](#).
- [30] A. Macridin, P. Spentzouris, J. Amundson, and R. Harnik, “Electron-Phonon Systems on a Universal Quantum Computer,” *Phys. Rev. Lett.* **121** no. 11, (2018) 110504, [arXiv:1802.07347 \[quant-ph\]](#).
- [31] H. Lamm and S. Lawrence, “Simulation of Nonequilibrium Dynamics on a Quantum Computer,” *Phys. Rev. Lett.* **121** no. 17, (2018) 170501, [arXiv:1806.06649 \[quant-ph\]](#).
- [32] N. Klco and M. J. Savage, “Digitization of scalar fields for quantum computing,” *Phys. Rev.* **A99** no. 5, (2019) 052335, [arXiv:1808.10378 \[quant-ph\]](#).
- [33] N. Klco, E. F. Dumitrescu, A. J. McCaskey, T. D. Morris, R. C. Pooser, M. Sanz, E. Solano, P. Lougovski, and M. J. Savage, “Quantum-classical computation of Schwinger model dynamics using quantum computers,” *Phys. Rev.* **A98** no. 3, (2018) 032331, [arXiv:1803.03326 \[quant-ph\]](#).
- [34] E. Gustafson, Y. Meurice, and J. Unmuth-Yockey, “Quantum simulation of scattering in the quantum Ising model,” *Phys. Rev.* **D99** no. 9, (2019) 094503, [arXiv:1901.05944 \[hep-lat\]](#).
- [35] NuQS Collaboration, A. Alexandru, P. F. Bedaque, H. Lamm, and S. Lawrence, “ σ Models on Quantum Computers,” *Phys. Rev. Lett.* **123** no. 9, (2019) 090501, [arXiv:1903.06577 \[hep-lat\]](#).
- [36] N. Klco and M. J. Savage, “Minimally-Entangled State Preparation of Localized Wavefunctions on Quantum Computers,” [arXiv:1904.10440 \[quant-ph\]](#).
- [37] N. Klco, J. R. Stryker, and M. J. Savage, “ $SU(2)$

- non-Abelian gauge field theory in one dimension on digital quantum computers,”
[arXiv:1908.06935 \[quant-ph\]](#).
- [38] NuQS Collaboration, H. Lamm, S. Lawrence, and Y. Yamauchi, “Parton Physics on a Quantum Computer,” [arXiv:1908.10439 \[hep-lat\]](#).
- [39] G. Magnifico, M. Dalmonte, P. Facchi, S. Pascazio, F. V. Pepe, and E. Ercolessi, “Real Time Dynamics and Confinement in the \mathbb{Z}_n Schwinger-Weyl lattice model for 1+1 QED,” [arXiv:1909.04821 \[quant-ph\]](#).
- [40] N. Mueller, A. Tarasov, and R. Venugopalan, “Deeply inelastic scattering structure functions on a hybrid quantum computer,” [arXiv:1908.07051 \[hep-th\]](#).
- [41] E. Gustafson, P. Dreher, Z. Hang, and Y. Meurice, “Real time evolution of a one-dimensional field theory on a 20 qubit machine,” [arXiv:1910.09478 \[hep-lat\]](#).
- [42] E. Zohar, J. I. Cirac, and B. Reznik, “Simulating Compact Quantum Electrodynamics with ultracold atoms: Probing confinement and nonperturbative effects,” *Phys. Rev. Lett.* **109** (2012) 125302, [arXiv:1204.6574 \[quant-ph\]](#).
- [43] D. Banerjee, M. Dalmonte, M. Muller, E. Rico, P. Stebler, U. J. Wiese, and P. Zoller, “Atomic Quantum Simulation of Dynamical Gauge Fields coupled to Fermionic Matter: From String Breaking to Evolution after a Quench,” *Phys. Rev. Lett.* **109** (2012) 175302, [arXiv:1205.6366 \[cond-mat.quant-gas\]](#).
- [44] E. Zohar, J. I. Cirac, and B. Reznik, “Cold-Atom Quantum Simulator for SU(2) Yang-Mills Lattice Gauge Theory,” *Phys. Rev. Lett.* **110** no. 12, (2013) 125304, [arXiv:1211.2241 \[quant-ph\]](#).
- [45] D. Banerjee, M. B C 6gli, M. Dalmonte, E. Rico, P. Stebler, U. J. Wiese, and P. Zoller, “Atomic Quantum Simulation of U(N) and SU(N) Non-Abelian Lattice Gauge Theories,” *Phys. Rev. Lett.* **110** no. 12, (2013) 125303, [arXiv:1211.2242 \[cond-mat.quant-gas\]](#).
- [46] U.-J. Wiese, “Ultracold Quantum Gases and Lattice Systems: Quantum Simulation of Lattice Gauge Theories,” *Annalen Phys.* **525** (2013) 777–796, [arXiv:1305.1602 \[quant-ph\]](#).
- [47] E. Zohar, J. I. Cirac, and B. Reznik, “Quantum Simulations of Lattice Gauge Theories using Ultracold Atoms in Optical Lattices,” *Rept. Prog. Phys.* **79** no. 1, (2016) 014401, [arXiv:1503.02312 \[quant-ph\]](#).
- [48] A. Bazavov, Y. Meurice, S.-W. Tsai, J. Unmuth-Yockey, and J. Zhang, “Gauge-invariant implementation of the Abelian Higgs model on optical lattices,” *Phys. Rev. D* **92** no. 7, (2015) 076003, [arXiv:1503.08354 \[hep-lat\]](#).
- [49] E. Zohar, A. Farace, B. Reznik, and J. I. Cirac, “Digital lattice gauge theories,” *Phys. Rev. A* **95** no. 2, (2017) 023604, [arXiv:1607.08121 \[quant-ph\]](#).
- [50] A. Bermudez, G. Aarts, and M. Muller, “Quantum sensors for the generating functional of interacting quantum field theories,” *Phys. Rev. X* **7** no. 4, (2017) 041012, [arXiv:1704.02877 \[quant-ph\]](#).
- [51] Bernien, H., Schwartz, S., Keesling, A. et al, “Probing many-body dynamics on a 51-atom quantum simulator,” *Nature* **551** (2017) 579584, [arXiv:1707.04344 \[quant-ph\]](#).
- [52] T. V. Zache, F. Hebenstreit, F. Jendrzewski, M. K. Oberthaler, J. Berges, and P. Hauke, “Quantum simulation of lattice gauge theories using Wilson fermions,” *Sci. Technol.* **3** (2018) 034010, [arXiv:1802.06704 \[cond-mat.quant-gas\]](#).
- [53] J. Zhang, J. Unmuth-Yockey, J. Zeiher, A. Bazavov, S. W. Tsai, and Y. Meurice, “Quantum simulation of the universal features of the Polyakov loop,” *Phys. Rev. Lett.* **121** no. 22, (2018) 223201, [arXiv:1803.11166 \[hep-lat\]](#).
- [54] H.-H. Lu *et al.*, “Simulations of Subatomic Many-Body Physics on a Quantum Frequency Processor,” *Phys. Rev. A* **100** no. 1, (2019) 012320, [arXiv:1810.03959 \[quant-ph\]](#).
- [55] F. M. Surace, P. P. Mazza, G. Giudici, A. Lerose, A. Gambassi and M. Dalmonte, “Lattice gauge theories and string dynamics in Rydberg atom quantum simulators,” [arXiv:1902.09551 \[cond-mat.quant-gas\]](#).
- [56] C. Kokail *et al.*, “Self-verifying variational quantum simulation of lattice models,” *Nature* **569** no. 7756, (2019) 355–360, [arXiv:1810.03421 \[quant-ph\]](#).
- [57] T. V. Zache, N. Mueller, J. T. Schneider, F. Jendrzewski, J. Berges and P. Hauke, “Dynamical Topological Transitions in the Massive Schwinger Model with a θ Term,” *Phys. Rev. Lett.* **122**, no. 5, (2019) 050403 , [arXiv:1808.07885 \[quant-ph\]](#).
- [58] L. Funcke, K. Jansen and S. Khn, “Topological vacuum structure of the Schwinger model with matrix product states,” [1908.00551 \[hep-lat\]](#).
- [59] C. J. Hamer, W.-h. Zheng, and J. Oitmaa, “Series expansions for the massive Schwinger model in Hamiltonian lattice theory,” *Phys. Rev. D* **56** (1997) 55–67, [arXiv:hep-lat/9701015 \[hep-lat\]](#).
- [60] K. Fujikawa, “Path Integral Measure for Gauge Invariant Fermion Theories,” *Phys. Rev. Lett.* **42** (1979) 1195–1198.
- [61] J. B. Kogut and L. Susskind, “Hamiltonian Formulation of Wilson’s Lattice Gauge Theories,” *Phys. Rev. D* **11** (1975) 395–408.
- [62] L. Susskind, “Lattice Fermions,” *Phys. Rev. D* **16** (1977) 3031–3039.
- [63] P. Jordan and E. Wigner, “Über das paulische äquivalenzverbot,” *Zeitschrift für Physik* **47** no. 9, (Sep, 1928) 631–651. <https://doi.org/10.1007/BF01331938>.
- [64] M. Luscher, “Computational Strategies in Lattice QCD,” in *Modern perspectives in lattice QCD*:

Quantum field theory and high performance computing. Proceedings, International School, 93rd Session, Les Houches, France, August 3-28, 2009, pp. 331–399. 2010. [arXiv:1002.4232 \[hep-lat\]](#).

- [65] M. C. Banuls, K. Cichy, K. Jansen, and H. Saito, “Chiral condensate in the Schwinger model with Matrix Product Operators,”

Phys. Rev. D **93** no. 9, (2016) 094512, [arXiv:1603.05002 \[hep-lat\]](#).

- [66] D. J. Gross, I. R. Klebanov, A. V. Matytsin, and A. V. Smilga, “Screening versus confinement in (1+1)-dimensions,” *Nucl. Phys.* **B461** (1996) 109–130, [arXiv:hep-th/9511104 \[hep-th\]](#).